Varied Coordination Geometries of an Alane/Tris(phosphine) Ligand from its Reactions with Pt(0) and Au(I)

*Samuel R. Lee, Brandy R. Adolph, Nattamai Bhuvanesh, and Oleg V. Ozerov**

Department of Chemistry, Texas A&M University, 3255 TAMU, College Station, TX 77842, USA.

ozerov@chem.tamu.edu

Abstract

Reactions of the tris(2-diisopropylphosphino-1-pyrrolyl)alane ligand **1** (AlP_3) furnished an (AlP_3)Pt complex **2**, which was determined to possess a Pt→Al interaction. Compound **2** reacted with CO to form the corresponding isolable adduct **3**. Exposure of **2** to H_2 or HD in solution resulted in the observation of equilibrium binding which favors **2** at room temperature, and more strongly favored the adducts **2-H_2** and **2-HD** at -80 °C. The presence of the Pt–H_2/HD moieties is supported by low temperature NMR determination of $^1J_{PPt}$ = 323 Hz (**2-H_2**) and $^1J_{HD}$ = 34 Hz (**2-HD**), ostensibly the first examples of Pt dihydrogen complexes with a trigonal bipyramidal geometry. The reaction of **1** with (tht)AuCl (tht = tetrahydrothiophene) generated compound **4** with loss of tht. An XRD study of **4** revealed the transfer of chloride to Al and a long separation between Al and Au coordinated by the three phosphine arms. Abstraction of chloride from **4** did not lead to a tripodal structure isoelectronic to **2**, but (according to solution NMR evidence) instead to the transfer of one of the phosphine arms to Al from Au in compound **5**.

1. Introduction

Ligands combining a central Lewis acid and three neutral donors (ZL_3 ligands) [1–3] are commonly explored to investigate the nature of the M→Z interactions, their influence on reactivity [4–6], and applications in catalysis [7–14]. The desired tripodal coordination of ZL_3 ligands to transition metal centers can be defined as **Type I** (Figure 1), with **A**, **B**, and **C** representing frequently studied frameworks [15–24]. The combination of a group 13 central Lewis acid [25] and three flanking phosphines is especially common. In the case of **E** (a congener of **B**-AuCl), coordination of the AlP_3 ligand is accompanied by chloride transfer to the Al center, affording what we term a **Type II** complex [26]. The preference for the coordination of the chloride to Al rather than Au and the absence of a strong Au→Al interaction is likely is a consequence of the high Lewis acidity of the Al center not being satisfied by the weak monovalent Au base. The Ga and In congeners of **E** adopt **Type II** structures, as well [27,28]. Our group recently reported the AlP_3 ligand **1** (Scheme 1), which furnished the **Type I** complex **D** with Ni, and exhibited a strong M→Al interaction [29]. However, ligand **1** afforded a **Type II** complex **F** in its reaction with AgOTf, and a **Type III** complex **G** in its reaction with $Ag[HCB_{11}Cl_{11}]$, where coordination of two phosphines and formation of an Al-P bond was observed [30]. The structures of **D** and **F** support the notion that ligand **1** (and related Al-centered ligands) can indeed adopt a **Type I** structure with a sufficiently basic transition metal partner such as d^{10} Ni(0), but not with a poor base such as d^{10} Ag(I).

Interrogation of the **B** series revealed M→B σ-donicity within group 10 decreased in the order of Au > Cu > Ag and Pt > Ni > Pd [18,19] . With that insight in hand, we set out to explore the analogs of D and F the 5d metals Pt and Au and report our findings herein.

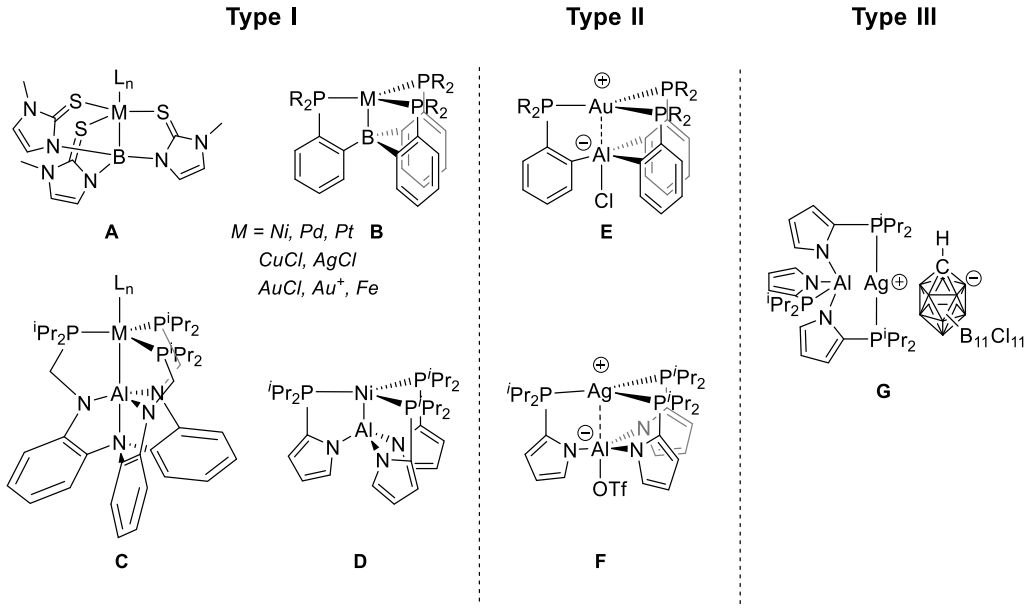

Figure 1. Representative types of complexes resulting from the interaction of ZL_3 ligands with late transition metals.

2. Results and Discussion.

2.1. *Synthesis and characterization of* ***Type I*** *AlP_3 complexes of Pt*

We first targeted the coordination of the AlP_3 ligand **1** with Pt (**Scheme 1**). Taking a cue from the synthesis of **B-Pt**, we utilized $(^tBu_3P)_2Pt$ as a convenient Pt(0) precursor. The reaction of **1** with $(^tBu_3P)_2Pt$ proceeded slowly, requiring thermolysis of a toluene solution for 5 days at 140 °C for completion, affording the desired product **2** in 73% yield upon workup. Introduction of an atmosphere of CO to a C_6D_6 solution of **2** afforded the adduct **3** quantitatively upon mixing. Removal of solvent under vacuum and redissolution in C_6D_6 under Ar atmosphere did not result in the loss of the Pt-bound CO.

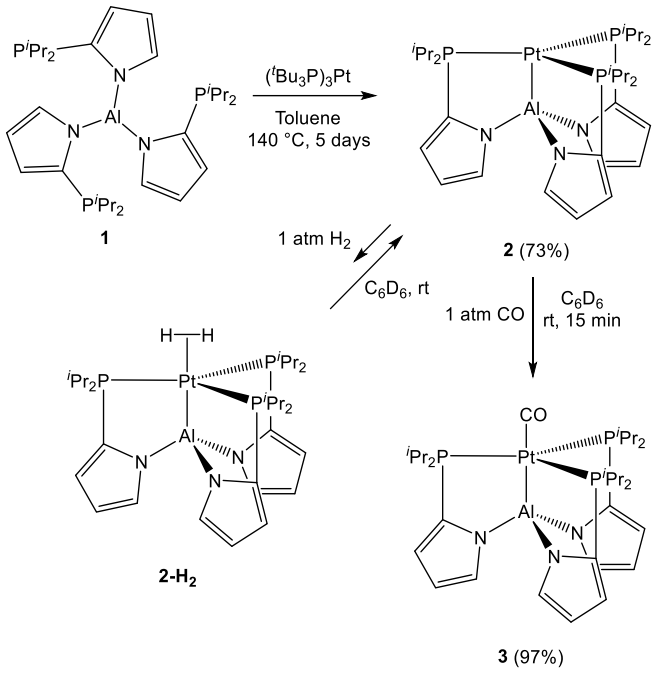

Scheme 1. Synthesis of Pt complexes of AlP_3 (**1**).

Compounds **2** and **3** exhibited apparent C_{3v} symmetry in their NMR spectra at ambient temperature. In the absence of crystallographic information, the **Type I** attachment of the AlP_3 ligand to Pt can be inferred from the value (**2**: 3056 Hz; **3**: 2901 Hz) of the $^1J_{P\text{-}Pt}$ coupling constant. It is significantly lower than the typical $^1J_{P\text{-}Pt}$ for the $(R_3P)_3Pt(0)$ complexes (ca. 4100-4500 Hz, e.g., **H**. Figure 2) **[31–34]**, but is similar to that in **J** (3032 Hz) **[33,34]**, suggesting a strong Pt→Al interaction. The $^1J_{P\text{-}Pt}$ value in **2** and **3** is considerably lower than in **B-Pt** (3578 Hz) **[19]**, but is higher than in the unambiguously Pt(II) compound **I** (2573, 2503 Hz) with a similar three-fold symmetric geometry **[35]**. The observed ν_{CO} = 1991 cm^{-1} for compound **3** can be compared to that in the various $(PR_3)_nPt(CO)$ complexes (ca. 1910 – 1930 cm^{-1}) **[36]**, including $(Ph_3P)_3PtCO$ (**K**), and to the complexes where CO is bound to a classical, square-planar Pt(II) center (ca. 2090-2120 cm^{-1}, **L** and **M**, Figure 2) **[37,38]**.

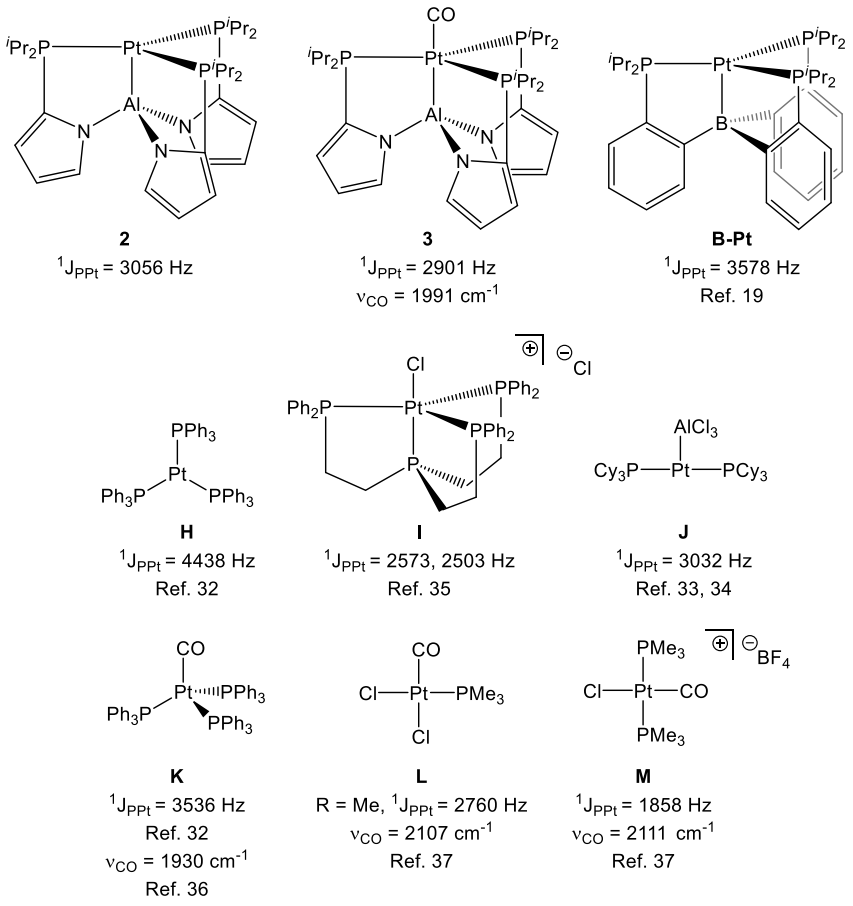

Figure 2. Comparison of the $^1J_{PPt}$ and ν(CO) values in literature examples vs **2** and **3.**

Complexes **2**, **3**, **B-Pt**, and $(Cy_3P)_2Pt–AlCl_3$ can be analyzed as arising from the coordination of a borane or alane Z-type ligand to the zerovalent L_nPt. For the sake of proper comparison, the chloroplatinum complexes **I**, **L**, and **M** can be analogously viewed as resulting from the formal addition of Cl^+ to L_nPt. Addition of a Z ligand or of Cl^+ engages a pair of electrons in the original d^{10} L_nPt fragment and renders it divalent and d^8 [2,3]. As should be expected, the $^1J_{P\text{-}Pt}$ and the ν_{CO} data show that the "addition" of Cl^+ results in greater depletion of electron density at Pt than the addition of a neutral alane or borane. The more electron-withdrawing $AlCl_3$ in **J** and tris(N-pyrrolyl)alane in **2** and **3** deplete the electron density at Pt (relative to L_nPt) to a greater degree than the triarylborane in **B-Pt**, and bring it closer along the electronic continuum to **I**, **L**,

and **M** than to L_nPt. We sought additional insight from electrochemical studies. With **D**, we observed well-behaved reduction and oxidation by cyclic voltammetry (CV). However, examination of compound **2** did not result in reversible reduction or oxidation events and the interpretation is not clear (see Supporting Information).

Given that **D** (as well as the Ga/In analogs of **C-Ni**), was shown to reversibly bind H_2, we explored the affinity of **2** for H_2 first by exposing it to an atmosphere of H_2 in C_6D_6 solution at ambient temperature. This caused broadening of the AlP_3 ^{1}H NMR signals, and the appearance of a broad signal at δ 3.39, which we surmised was indicative of a rapid equilibrium between free H_2 (with unbound **2**) and a Pt–H_2 complex **2-H_2**. We then treated a solution of **2** in toluene-d_8 with 1 atm H_2 and examined the ^{1}H NMR spectra of this solution from 25 °C to -80 °C. At 25 °C, the time-averaged H_2/Pt–H_2 signal appeared at δ 3.62. The H_2 signal shifted upfield with decreasing temperature (ca. 2.91 ppm at 10 °C, -0.63 ppm at -30 °C), terminating with δ -1.55 at -80 °C. At temperatures in the -60 °C to -80 °C range, the broad H_2/Pt–H_2 signal displayed ^{195}Pt satellites, with $^1J_{HPt} \approx 323$ Hz at -80 °C, consistent with the few previously reported observations of Pt–H_2 complexes **[39–42]**.

Seeking to confirm this observation as a Pt–H_2 complex, we studied the addition of a mixture of HD and H_2 (generated by reaction of CaH_2 and D_2O) to a solution of **2** in toluene-d_8. The broadened signals for **2** were reproduced, alongside a broad signal at δ 4.26, representing the time-averages for H_2/Pt–H_2 and HD/Pt–HD. We examined the ^{1}H NMR spectra of the solution from 25 °C to -80 °C under HD/H_2 atmosphere. Upon cooling, the signal at δ 4.26 (25 °C) resolved into individual signals corresponding to H_2/Pt–H_2 and HD/Pt–HD, both of which shifted upfield with the decrease in temperature. At -10 °C and below, H_2 (δ 3.19) and HD (δ 3.01, $^1J_{HD} = 39$ Hz) were

fully resolved. At -80 °C, two overlapping but distinct signals at ca. δ -1.5 (J_{HD} = 34 Hz) were observed.

Since we did not observe a signal for the uncoordinated H_2 or HD at – 80 °C, the resonances at δ -1.5 may still represent a weighted average of free H_2/HD and **2-H₂**/**2-HD**. However, it seems likely that it is predominantly the latter and the J_{HD} coupling constant indicates a dihydrogen complex with only modest perturbation of H-D bonding **[43,44]**. **D** displayed similar affinity for H_2, with only partial binding at ambient temperature, and a similar J_{HD} = 35 Hz coupling constant was determined at low temperature. Dihydrogen complexes of Pt are relatively rare, and limited to square planar Pt(II) species with strongly *trans*-influencing ligands opposite the H_2 ligand **[39–42,45]**. To our knowledge, the low temperature observation of **2-H₂** is the first for a dihydrogen complex of Pt in a trigonal-bipyramidal geometry. For an example of an isolobal trigonal-bypiramidal Co–H_2 complex, see the related **[K(THF)ₙ][B-Co-H₂]**, which features a more activated dihydrogen moiety (J_{HD} = 29 Hz in the HD analog) **[46]**.

2.2. *Synthesis and characterization of **Types II** and **III** AlP_3 complexes of Au(I)*

Next, we examined the formation of Au complexes supported by **1**. Addition of (tht)AuCl to a toluene solution of **1** afforded **4** upon mixing at ambient temperature. **4** was isolated in 64% yield after workup. Compound **4** displayed a single resonance by $^{31}P\{^1H\}$ NMR spectroscopy at δ 42.4 and a decreased C_3 symmetry in its ^1H and $^{13}C\{^1H\}$ NMR spectra. Among the four chemically inequivalent ^1H NMR resonances corresponding to the Me groups, one was distinguished by an unusual δ -0.06 ppm chemical shift, likely arising from the ring current effect of the neighboring aromatic ring(s). X-ray structural analysis of **4** established that coordination of the phosphines of **1** to Au is coupled with a chloride transfer to Al (*vide infra*), generating the **Type II** zwitterion analogous to **E** and **F**.

Reaction of **4** with $Na[CHB_{11}Cl_{11}]$ in PhF solution proceeded cleanly via chloride abstraction within 1 h at ambient temperature, generating **5** in 88% yield upon workup. However, instead of the **Type I** structure isoelectronic to **2**, the $^{31}P\{^{1}H\}$ NMR analysis suggested the **Type III** motif for **5**, with two ^{31}P NMR resonances in a 2:1 ratio (δ 53.2, -1.3). The ^{1}H NMR spectrum also showed a 2:1 ratio of unique pyrrolyl signals. The unique ^{31}P NMR resonance in **G**, corresponding to the Al-bound P, displayed a very similar chemical shift of δ -1.8 ppm. Based on these observations, we believe that the structure of **5** is analogous to that of **G**.

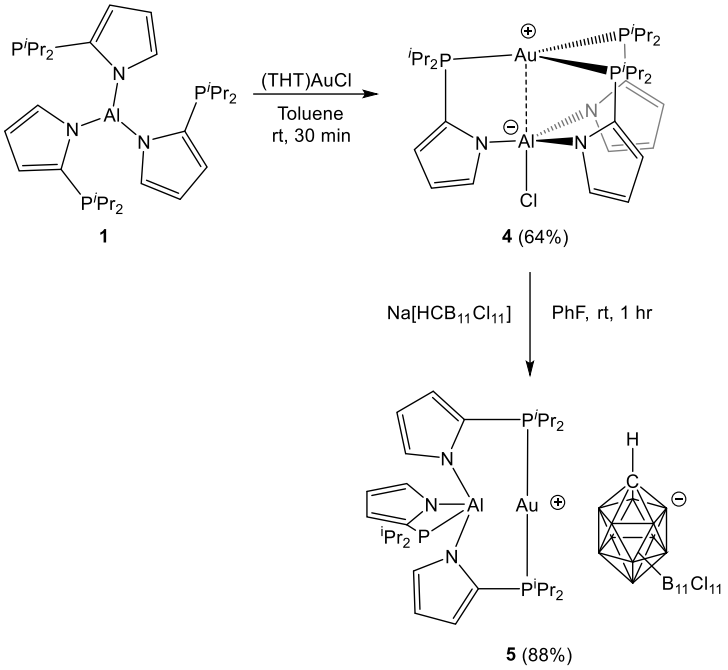

Scheme 2. Synthesis of Au complexes of AlP_3 (**1**).

2.3. *Structural Study of **4***

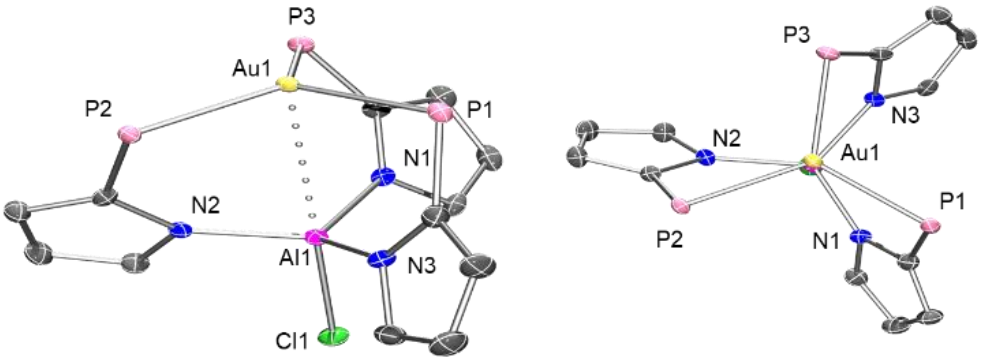

Figure 3. *POV-ray renditions of the ORTEP drawing (50% thermal ellipsoids) of **3** showing selected atom labelling. Hydrogen atoms, isopropyl groups, and solvent atoms omitted for clarity. Selected bond distances (Å) and angles (°): Au1–Al1, 3.1177(18); Al1–Cl1, 2.181(2); Au1–P1, 2.3667(16); Au1–P2, 2.3713(17); Au1–P3, 2.3732(15); Al1–N1, 1.900(6); Al1–N2, 1.897(6); Al1–N3, 1.900(5); P1 – Au1 – P2, 118.73(5) ; P1 – Au1 – P3, 119.53(6) ; P2 – Au1 – P3, 119.15(6) ; N1 – Al1 – N2, 118.8(3) ; N1 – Al1 – N3, 114.7(3) ; N2 – Al1 – N3, 117.0(2); N1 – Al1 – Cl1, 79.01(18) ; N2 – Al1 – Cl1, 80.22(18); N3 – Al1 – Cl1, 79.79(18); Au1 – Al1 – N1, 99.90(17); Au1 – Al1 – N2, 100.23(16); Au1 – Al1 – N3, 100.85(17); Au1 – Al1 – Cl1, 178.90(9).*

Single crystals of **4** were grown from a saturated Et_2O solution at -35 °C and subjected to an XRD study (**Figure 4**), which established a **Type II** structure reminiscent of **E** and **F** [26,30]. The geometry about Au is approximately trigonal planar with the sum of P–Au–P bond angles equal to ca. 357.4°, with Au sitting slightly out of the plane defined by P,P,P with a distance of ca. 0.22 Å (cf. 0.14 Å in **E**, 0.32 Å in **F**) [26,30], and away from Al. The chloroaluminate fragment adopts a pyramidal structure pointed away from the Au^+ center, with the sum of N–Al–N bond angles being ca. 350.5°, and Al sits out of the plane defined by N,N,N with a distance of ca. 0.34 Å (cf. 0.29 Å to C,C,C plane in **E**, 0.30 Å to N,N,N plane in **F**) [26,30]. The Cl, Al, and Au atoms are nearly on a straight line (Au–Al–Cl angle 178.9°). The Au–Al distance of 3.12 Å is smaller than the sum of van der Waals radii (4.2 Å), but is considerably larger than the sum of covalent radii (2.57 Å) [47,48]. This value is similar to the Ag-Al distance in **F** (ca. 3.18 Å; Ag and Au are

of essentially the same size) and longer than the Au-Al distance (3.03 Å) in **E** [26]. On the whole, the Au-Al interaction, if any, should be very weak.

3. Conclusions

In summary, we were able to explore the coordination of the AlP_3 ligand **1** to zerovalent Pt and monovalent Au, the metals of the 5d series. Similarly to the interactions of **1** with Ni we explored previously [29], we found that the relatively electron-rich group 10 metal Pt readily forms a tripodal structure in which **1** acts as a ZL_3 ligand towards Pt and enables Pt to coordinate H_2 and CO. Spectroscopic data suggest a strong Pt→Al interaction consistent with the tris(N-pyrrolyl)aluminum moiety acting as a strong Lewis acid towards the Pt base. With AuCl or Au^+, ligand **1** formed complexes devoid of the strong Au→Al interaction, similarly paralleling the observations with AgOTf and Ag^+ [30]. In these complexes, Al prefers to bind either a chloride, or one of the phosphine arms, demonstrating that even a 5d congener in group 11 is not a strong enough base to attract an aluminum Lewis acid in AlP_3 ligand **1**.

4. Experimental

4.1 **General Considerations.** Unless specified otherwise, all manipulations were performed under an Ar atmosphere using standard Schlenk line or glovebox techniques. Toluene, diethyl ether, isooctane, and pentane were dried and deoxygenated (by sparging with argon) using an Innovative Technologies MD-5 solvent purification system and stored over molecular sieves in an Ar-filled glovebox. Toluene-d_8, C_6D_6, $CDCl_3$, CD_2Cl_2, and fluorobenzene (PhF) were dried over CaH_2. The solvents were distilled or vacuum transferred and stored over molecular sieves in an Ar-filled glovebox. Ligand **1** [29] and $[Na][CHB_{11}Cl_{11}]$ [49] were synthesized according to literature precedent. All other chemicals were used as received from commercial vendors. NMR spectra were recorded on Bruker Avance Neo 400 (^{1}H NMR, 400.200 MHz; ^{13}C NMR, 100.630 MHz; ^{31}P NMR, 161.95 MHz), Inova 500 (^{1}H NMR, 499.431 MHz; ^{13}C NMR, 125.595 MHz; ^{31}P NMR, 202.187

MHz), and Avance Neo 500 (^{1}H NMR, 500.13 MHz; ^{13}C NMR, 125.77 MHz; ^{31}P NMR, 202.45 MHz) spectrometers. Chemical shifts are reported in δ (ppm). For ^{1}H and ^{13}C NMR spectra, the residual solvent peak was used as an internal reference (^{1}H NMR: δ 7.16 for C_6D_6, 2.08 for toluene-d_8, 7.26 for $CDCl_3$, 5.32 for CD_2Cl_2; ^{13}C NMR: δ 128.06 for C_6D_6, 77.16 for $CDCl_3$, 53.84 for CD_2Cl_2). ^{31}P NMR spectra were externally referenced to an 85% phosphoric acid solution δ 0.00. Elemental analyses were performed by Eutech Scientific Services (Mount Olive, NJ) and Robertson Microlit Laboratories (Ledgewood, NJ).

4.2. **Synthesis of AlP_3M Complexes**

Synthesis of 2. To a screw-cap test tube charged with stir bar and a solution containing 129 mg of **1** (0.225 mmol) in 4 mL of toluene, 135 mg of (^{t}Bu$_3$P)$_2$Pt (0.225 mmol) was added. The test tube was sealed and placed in a 140 °C oil bath for 5 days with stirring, resulting in a dark red solution. The volatiles were evaporated, and the residue washed with cold pentane (2 mL ×3) to afford an orange-red powder (126 mg, 73%). ^{1}H NMR (C_6D_6, 500 MHz): δ 7.09 (brs, Pyrrolyl-*H*, 3H), 6.64 (m, Pyrrolyl-*H*, 3H), 6.58 (m, Pyrrolyl-*H*, 3H), 2.73 (m, C*H*Me$_2$, 6H), 1.06 (m, CH*Me$_2$*, 18H), 0.89 (m, CH*Me$_2$*, 18H). ^{1}H NMR (Toluene-d_8, 400 MHz): δ 7.02 (brs, Pyrrolyl-*H* 3H), 6.56 (d, J = 3 Hz, Pyrrolyl-*H*, 3H), 6.47 (m, Pyrrolyl-*H*, 3H), 2.71 (m, C*H*Me$_2$, 6H), 1.04 (m, CH*Me$_2$*, 18H), 0.87 (m, CH*Me$_2$*, 18H). ^{13}C{^{1}H} NMR (C_6D_6, 101 MHz): δ 132.1 (m, Pyrrolyl-*C*), 126.4 (br m, Pyrrolyl-*C*), 114.6 (t, $J_{C\text{-}P}$ = 11.4 Hz), 112.9 (t, $J_{C\text{-}P}$ = 8.0 Hz, Pyrrolyl-*C*), 32.1 (m, *C*HMe$_2$), 20.0 (CH*Me$_2$*), 19.4 (CH*Me$_2$*). ^{31}P{^{1}H} NMR (202 MHz) δ 63.2 ($^1J_{P\text{-}Pt}$ = 3056 Hz). Elem. Anal. Calcd for $C_{30}H_{51}AlN_3P_3Pt$: C, 46.87; H, 6.69; N, 5.47. Found: C, 46.56; H, 7.09; N, 5.30.

Reaction of 2 with H_2. To a J. Young tube, 20.2 mg of **2** (0.026 mmol) was loaded with 0.6 mL C_6D_6. The solution was degassed via freeze-pump-thaw cycles then back filled with 1 atm H_2. No color change was observed, and after 15 minutes ^{1}H and ^{31}P{^{1}H} NMR were collected. In both the ^{1}H and ^{31}P{^{1}H} spectra, resonances corresponding to **2** appeared slightly broadened, with a signal

corresponding to a time-average of H_2 and Pt–H_2. After 24 hours under 1 atm H_2, the ^{1}H NMR signals were observed to have sharpened, with a slight shift in the H_2/Pt–H_2 time-averaged signal. *Reactions involving refill with H_2 often introduce impurities which cause partial decomposition (likely adventitious water). After 18 hours under H_2, 10% decomposition is observed by $^{31}P\{^1H\}$ NMR integration, with accompanying impurity signals in the upfield ^1H NMR region (see* ***Figures S8 and S7****, respectively in Supplementary Information).* ^{1}H NMR (C_6D_6, 500 MHz, 298 K) δ 7.09 (brs, Pyrrolyl-*H*, 3H), 6.64 (m, Pyrrolyl-*H*, 3H), 6.58 (m, Pyrrolyl-*H*, 3H), 3.39 (brs, *time-averaged H_2,* 0.13H,) 2.72 (m, C*H*Me_2, 6H), 1.05 (m, CHMe_2, 18H), 0.90 (m, CH*Me_2*, 18H). ^{31}P{^{1}H} NMR (C_6D_6, 202 MHz, 298 K) δ 63.2 ($^1J_{PPt}$ = 3059 Hz).

Variable Temperature NMR Study of the Reaction of 2 with H_2. A J. Young NMR tube containing 15 mg **2** (0.02 mmol) in 0.5 mL toluene-*d8* was degassed and refilled with 1 atm H_2 followed by vigorous shaking. Variable temperature NMR spectra were recorded observing ^{1}H on a Bruker Avance Neo 500 spectrometer from 25 °C to -80 °C. ^{1}H NMR (Toluene-*d8*, 500 MHz, 298 K) δ 7.02 (brs, Pyrrolyl-*H*, 3H), 6.55 (d, *J* = 3 Hz, Pyrrolyl-*H*, 3H), 6.47 (m, Pyrrolyl-*H*, 3H), 3.46 (s, time-averaged *H_2*/Pt–*H_2*, 0.15H), 2.69 (m, C*H*Me_2, 6H), 1.03 (m, CH*Me_2*, 18H), 0.87 (m, CH*Me_2*, 18H). ^{1}H NMR (Toluene-*d_8*, 500 MHz, 273 K, *H_2/Pt–H_2 time-average*) δ 2.92 (0.47H). ^{1}H NMR (Toluene-*d_8*, 500 MHz, 233 K, *H_2/Pt–H_2 time-average*) δ -0.64 (0.48H). ^{1}H NMR (Toluene-*d_8*, 500 MHz, 183 K, *H_2/Pt–H_2 time-average*) δ -1.55 ($^1J_{HPt}$ = 323 Hz, 1.80H). *Reactions involving refill with H_2 often introduce impurities which cause partial decomposition (likely adventitious water). The NMR signals corresponding to decomposition did not interfere with the VT studies.*

Reaction of 2 with HD and Variable Temperature NMR Study. A 1000 mL PTFE stoppered round bottom Schlenk flask was charged with 2.1 g CaH_2 (49.9 mmol) under a stream of argon. The flask was placed in a liquid N_2 bath and cooled for 10 minutes before addition of 1.2 mL D_2O (66 mmol) under a stream of argon. The headspace was removed under vacuum for 10 minutes before the flask was removed from the cooling bath. The flask was thawed while connected to a single manifold gas line fitted with a pressure gauge until 1 atm was generated. A J. Young tube

containing 10 mg **2** (0.01 mmol) in 0.5 mL toluene-d_8 was degassed via 2 cycles of freeze-pump-thaw and refilled with 1 atm of the HD/H_2 mixture. The tube was shaken vigorously, and the color of the solution changed from red to red-orange. Variable temperature NMR spectra were recorded observing ^{1}H on a Bruker Avance Neo 500 spectrometer from 25 °C to -80 °C. *Reactions involving refill with HD/H_2 often introduce impurities which cause partial decomposition (likely adventitious water). The NMR signals corresponding to decomposition did not interfere with the VT studies.*

Synthesis of 3. To a J. Young tube, 20.2 mg of **2** (0.026 mmol) was added and dissolved in 0.5 mL C_6D_6. The solution was degassed via 3 freeze-pump-thaw cycles and back filled with 1 atm CO before stirring for 15 minutes to reveal **3** as the sole product by ^{1}H and ^{31}P NMR. The solution was transferred to a vial and lyophilized to give 20 mg of **3** (97 %). The sample was redissolved in C_6D_6 to confirm via multinuclear NMR the retention of CO. ^{1}H NMR (C_6D_6, 500 MHz): δ 7.25 (brs, Pyrrolyl-*H*, 3H), 6.72 (brs, Pyrrolyl-*H*, 3H), 6.52 (brs, Pyrrolyl-*H*, 3H), 2.12 (m, C*H*$(CH_3)_2$, 6H), 0.95 (m, CH(C*H*$_3)_2$, 18H), 0.52 (m, CH(C*H*$_3)_2$, 18H). ^{13}C{^{1}H} NMR (C_6D_6, 125 MHz): δ 114.5 (ovlp signals, Pyrrolyl-*C*), 114.2 (Pyrrolyl-*C*), 28.9 (*C*HMe$_2$, 18.7 (CH*Me*$_2$), 17.4 (CH*Me*$_2$). ^{31}P{^{1}H} NMR (202 MHz) δ 7.2 ($^1J_{P\text{-}Pt}$ = 2901 Hz). IR, ν_{CO} 1991.3 cm^{-1}. *The $^{13}C\{^1H\}$ signal corresponding to Pt-CO was not detected, likely a consequence of its broadness and multiplicity.*

Synthesis of 4. To a 20 mL scintillation vial charged with 37.1 mg (tht)AuCl (0.116 mmol) and stir bar, a 2 mL toluene solution containing 66.4 mg of **1** (0.116 mmol) was added and stirred in the dark for 5 minutes at room temperature. Volatiles were then evaporated, and the resulting residue dissolved in 0.5 mL Et_2O and cooled to -35 °C overnight, affording 60.1 mg (64%) of **4** as a colorless crystal. Single crystals suitable for X-ray crystallography were obtained from a concentrated Et_2O solution cooled to -35 °C overnight. ^{1}H NMR (500 MHz, $CDCl_3$) δ 7.89 (br s, Pyrrolyl-*H*, 3H), 6.42 (m, Pyrrolyl-*H*, 3H), 6.21 (m, Pyrrolyl-*H*, 3H), 2.98 (m, C*H*Me$_2$, 3H), 1.99 (m, C*H*Me$_2$, 3H), 1.25 (m, CH*Me*$_2$, 9H), 1.18 (m, CH*Me*$_2$, 9H), 1.08 (m, CH*Me*$_2$, 9H), -0.06 (m, CH*Me*$_2$, 9H). ^{13}C{^{1}H} NMR (126 MHz, $CDCl_3$) δ 138.3 (Pyrrolyl-*C*), 120.2 (Pyrrolyl-*C*), 110.3

(Pyrrolyl-*C*), 109.9 (Pyrrolyl-*C*), 26.31 (ovlp. m, *C*HMe$_2$), 21.1 (CH*Me$_2$*), 19.8 (CH*Me$_2$*), 16.8 (CH*Me$_2$*), 16.1 (CH*Me$_2$*). $^{31}P\{^1H\}$ NMR ($CDCl_3$, 202 MHz) δ 43.0. Elem. Anal. Calcd for $C_{30}H_{51}AlAuClN_3P_3$: C, 44.70; H, 6.38; N, 5.21. Found: C, 44.68; H, 6.42; N, 4.89.

Synthesis of 5. A 25 mL Schlenk flask was charged with 101 mg **3** (0.125 mmol) before a solution containing 68 mg $Na[HCB_{11}Cl_{11}]$ in 5 mL PhF was added with stirring for 1 hour in the dark. The resulting suspension was filtered through a short pad of celite and volatiles were removed to give 143 mg **5** as a light yellow powder (88%). This powder was dissolved in minimal PhF and the solution layered with isooctane and stored overnight in a -35 C freezer. The resulting yellow powder was captured on a medium porosity fritted filter, washed 3 times with 2 mL of cold pentane, and dried under vacuum, giving 117 mg of **5**×$(PhF)_{0.5}$ (70%) (Figure **S**). ^1H NMR (400 MHz, CD_2Cl_2) δ 7.62 (s, *Pyrrolyl-*H*, 1H), 7.44 (s, Pyrrolyl-*H*, 2H), 6.72 (m, Pyrrolyl-*H*, 4H), 6.62 (m, *Pyrrolyl-*H*, 2H), 3.23 (brs, C*H*$B_{11}Cl_{11}$, 1H), 3.12 (m, C*H*Me$_2$, 2H), 2.49 (m, C*H*Me$_2$, 2H), 2.26 (m, *C*H*Me$_2$, 2H,), 1.43 (m, CH*Me$_2$*, 6H), 1.22-1.07 (ovlp. m, CH*Me$_2$*, 18H), 0.96-0.88 (ovlp. m, CH*Me$_2$*, 12H). $^{13}C\{^1H\}$ NMR (126 MHz, CD_2Cl_2) δ 132.8 (m, Pyrrolyl-*C*), 130.4 (d, Pyrrolyl-*C*, $J_{C\text{-}P}$ = 7.8 Hz), 129.9 (d, Pyrrolyl-*C*, $J_{C\text{-}P}$ = 19.4 Hz), 122.10 (Pyrrolyl-*C*), 118.6 (m, Pyrrolyl-*C*), 117.3 (m, Pyrrolyl-*C*), 115.5 (d, Pyrrolyl-*C*, $J_{C\text{-}P}$ = 21.0 Hz), 115.0 (Pyrrolyl-*C*), 47.5 (*C*H$B_{11}Cl_{11}$), 28.5 (t, *C*HMe$_2$, $J_{C\text{-}P}$ = 16.8 Hz), 27.5 (t, *C*HMe$_2$, $J_{C\text{-}P}$ = 18.8 Hz), 23.0 (d, **C*HMe$_2$, $J_{C\text{-}P}$ = 22.9 Hz), 20.9 (CH*Me$_2$*), 20.5 (CH*Me$_2$*), 18.7 (CH*Me$_2$*), 18.2 (CH*Me$_2$*), 17.9 (d, *CH*Me$_2$*, $J_{C\text{-}P}$ = 3.2 Hz), 17.6 (CH*Me$_2$*). $^{31}P\{^1H\}$ NMR (CD_2Cl_2, 162 MHz) δ 53.2 (s, 2P), -1.3 (brs, 1P*). Elem. Anal. Calcd for $C_{31}H_{52}AlAuB_{11}Cl_{11}N_3P_3$×$(C_6H_5F)_{0.5}$: C, 30.46; H, 4.10; N, 3.13. Found: C, 30.17; H, 4.11; N, 2.95.

4.3 **X-Ray data collection, solution, and refinement for compound 4 (CCDC 2354172).**

A Leica M80 microscope was used to identify a suitable single colourless block-shaped crystal of **3** showing well defined faces with dimensions 0.51 × 0.38 × 0.28 mm^3 from a

representative sample of crystals of the same habit. The crystal mounted on a nylon loop was then placed in a cold nitrogen stream (Oxford) maintained at T = 110.00 K.

Crystal screening, unit cell determination, and data collection were carried out using a Bruker Quest (PHOTON III) diffractometer. The diffraction pattern was indexed and the total number of runs and images was based on the strategy calculation from the program APEX 4 [50]. Data were measured using *f* and *w* scans with MoK_a radiation. Data was collected to a maximum resolution of Q = 30.249° (0.71 Å). The unit cell was refined using SAINT V8.40B [51] on 9608 reflections, 19 % of the observed reflections.

Integrated Intensity information for each reflection was obtained by reduction of data frames using SAINT V8.40B [51]. The final completeness is 99.50 % out to 30.249° in Q. SADABS-2016/2 [51] was used for absorption correction. wR_2(int) was 0.1259 before and 0.0580 after correction. The Ratio of minimum to maximum transmission is 0.3118. The l/2 correction factor is Not present. The absorption coefficient m of this material is 3.943 mm^{-1} at this wavelength (l = 0.71073Å) and the minimum and maximum transmissions are 0.037 and 0.118.

Systematic reflection conditions and statistical tests of the data suggested the space group $P2_1/c$ (# 14) and was confirmed by XT [52] structure solution program using dual methods. The structure was refined by full matrix least squares minimisation on $\boldsymbol{F^2}$ using version 2018/3 of XL [53]. All non-hydrogen atoms were refined anisotropically. Hydrogen atom positions were calculated geometrically and refined using the riding model.

4.4. **Electrochemical Analysis**

Electrochemical studies were carried out using a CH Instruments Model 700 D Series. Electrochemical Analyzer and Workstation in conjunction with a three-electrode cell. The working electrode was a CHI 104 glassy carbon disk with a 3.0 mm diameter and the auxiliary electrode was composed of platinum wire. The third electrode, the reference electrode, was a $Ag/AgNO_3$ electrode. This was prepared as a bulk solution composed of 0.01 M $AgNO_3$ and 0.2 M $[^nBu_4N][BArF_{24}]$ in fluorobenzene. This was separated from solution by a fine porosity frit. CVs

were conducted in fluorobenzene with 0.2 M [$^{n}Bu_4N$][$BArF_{24}$] as supporting electrolyte and were reported with a scan rate of 100 mV/s. The concentration of the analyte solutions were approximately 1.00×10^{-3} M. CVs were referenced to $Fe(\eta\text{-}Cp)_2^{+}$/ $Fe(\eta\text{-}Cp)_2$ redox couple.

Appendix A. Supplementary data.

Supplementary data to this article containing graphical spectral data, and the details of X-ray structure determinations can be found online. CCDC 2354172 contains the supplementary crystallographic data for compound **4**. These data can be obtained free of charge via http://www.ccdc.cam.ac.uk/conts/retrieving.html, or from the Cambridge Crystallographic Data Centre, 12 Union Road, Cambridge CB2 1EZ, UK; fax: (+44) 1223-336-033; or e-mail: deposit@ccdc.cam.ac.uk.

Acknowledgments. We are grateful for the support of this work by the US National Science Foundation (grant CHE-2102324 to O.V.O.). We thank Prof. Jia Zhou for performing preliminary DFT calculations on related structures that helped delineate the scope of this work.

References.

[1] M.L.H. Green, G. Parkin, Application of the Covalent Bond Classification Method for the Teaching of Inorganic Chemistry, J. Chem. Educ. 91 (2014) 807–816. https://doi.org/10.1021/ed400504f.

[2] G. Parkin, A Simple Description of the Bonding in Transition-Metal Borane Complexes, Organometallics 25 (2006) 4744–4747. https://doi.org/10.1021/om060580u.

[3] G. Parkin, Impact of the coordination of multiple Lewis acid functions on the electronic structure and vn configuration of a metal center, Dalton Trans. 51 (2022) 411–427. https://doi.org/10.1039/D1DT02921E.

[4] A. Amgoune, D. Bourissou, σ-Acceptor, Z-type ligands for transition metals, Chem. Commun. 47 (2010) 859–871. https://doi.org/10.1039/C0CC04109B.

[5] B.J. Graziano, T.R. Scott, M.V. Vollmer, M.J. Dorantes, V.G. Young, E. Bill, L. Gagliardi, C.C. Lu, One-electron bonds in copper–aluminum and copper–gallium complexes, Chem. Sci. 13 (2022) 6525–6531. https://doi.org/10.1039/D2SC01998A.

[6] J.R. Prat, R.C. Cammarota, B.J. Graziano, J.T. Moore, C.C. Lu, Toggling the Z-type interaction off-on in nickel-boron dihydrogen and anionic hydride complexes, Chem. Commun. 58 (2022) 8798–8801. https://doi.org/10.1039/D2CC03219H.

[7] D. You, F.P. Gabbaï, Tunable σ-Accepting, Z-Type Ligands for Organometallic Catalysis, Trends in Chemistry 1 (2019) 485–496. https://doi.org/10.1016/j.trechm.2019.03.011.

[8] R.C. Cammarota, M.V. Vollmer, J. Xie, J. Ye, J.C. Linehan, S.A. Burgess, A.M. Appel, L. Gagliardi, C.C. Lu, A Bimetallic Nickel–Gallium Complex Catalyzes CO2 Hydrogenation via the Intermediacy of an Anionic d10 Nickel Hydride, J. Am. Chem. Soc. 139 (2017) 14244–14250. https://doi.org/10.1021/jacs.7b07911.

[9] J.S. Anderson, J. Rittle, J.C. Peters, Catalytic conversion of nitrogen to ammonia by an iron model complex, Nature 501 (2013) 84–87. https://doi.org/10.1038/nature12435.

[10] J.T. Moore, C.C. Lu, Catalytic Hydrogenolysis of Aryl C–F Bonds Using a Bimetallic Rhodium–Indium Complex, J. Am. Chem. Soc. 142 (2020) 11641–11646. https://doi.org/10.1021/jacs.0c04937.

[11] J.T. Moore, M.J. Dorantes, Z. Pengmei, T.M. Schwartz, J. Schaffner, S.L. Apps, C.A. Gaggioli, U. Das, L. Gagliardi, D.A. Blank, C.C. Lu, Light-Driven Hydrodefluorination of Electron-Rich Aryl Fluorides by an Anionic Rhodium-Gallium Photoredox Catalyst, Angewandte Chemie International Edition 61 (2022) e202205575. https://doi.org/10.1002/anie.202205575.

[12] D.J. Schild, L. Nurdin, M.-E. Moret, P.H. Oyala, J.C. Peters, Characterization of a Proposed Terminal Iron(III) Nitride Intermediate of Nitrogen Fixation Stabilized by a Trisphosphine-Borane Ligand, Angewandte Chemie International Edition 61 (2022) e202209655. https://doi.org/10.1002/anie.202209655.

[13] M.V. Vollmer, J. Xie, C.C. Lu, Stable Dihydrogen Complexes of Cobalt(−I) Suggest an Inverse trans-Influence of Lewis Acidic Group 13 Metalloligands, J. Am. Chem. Soc. 139 (2017) 6570–6573. https://doi.org/10.1021/jacs.7b02870.

[14] W.H. Harman, T.-P. Lin, J.C. Peters, A d10 Ni–(H2) Adduct as an Intermediate in H□H Oxidative Addition across a Ni□B Bond, Angewandte Chemie International Edition 53 (2014) 1081–1086. https://doi.org/10.1002/anie.201308175.

[15] M.R.St.-J. Foreman, A.F. Hill, P. White, D.J. Williams, Polyazolyl Chelate Chemistry. 13. An Osmaboratrane1, Organometallics 23 (2004) 913–916. https://doi.org/10.1021/om0306123.

[16] D. J. Mihalcik, J. L. White, J. M. Tanski, L. N. Zakharov, G.P. A. Yap, C. D. Incarvito, A. L. Rheingold, D. Rabinovich, Cobalt tris(mercaptoimidazolyl)borate complexes: synthetic studies and the structure of the first cobaltaboratrane, Dalton Transactions 0 (2004) 1626–1634. https://doi.org/10.1039/B401056F.
[17] K. Pang, J.M. Tanski, G. Parkin, Reactivity of the Ni→B dative σ-bond in the nickel boratrane compounds [κ4-B(mimBut)3]NiX (X = Cl, OAc, NCS, N3): synthesis of a series of B-functionalized tris(2-mercapto-1-tert-butylimidazolyl)borato complexes, [YTmBut]NiZ, Chem. Commun. (2008) 1008–1010. https://doi.org/10.1039/B714466K.
[18] M. Sircoglou, S. Bontemps, G. Bouhadir, N. Saffon, K. Miqueu, W. Gu, M. Mercy, C.-H. Chen, B.M. Foxman, L. Maron, O.V. Ozerov, D. Bourissou, Group 10 and 11 Metal Boratranes (Ni, Pd, Pt, CuCl, AgCl, AuCl, and Au+) Derived from a Triphosphine−Borane, J. Am. Chem. Soc. 130 (2008) 16729–16738. https://doi.org/10.1021/ja8070072.
[19] S. Bontemps, G. Bouhadir, W. Gu, M. Mercy, C.-H. Chen, B.M. Foxman, L. Maron, O.V. Ozerov, D. Bourissou, Metallaboratranes Derived from a Triphosphanyl–Borane: Intrinsic C3 Symmetry Supported by a Z-Type Ligand, Angewandte Chemie International Edition 47 (2008) 1481–1484. https://doi.org/10.1002/anie.200705024.
[20] M.-E. Moret, L. Zhang, J.C. Peters, A Polar Copper–Boron One-Electron σ-Bond, J. Am. Chem. Soc. 135 (2013) 3792–3795. https://doi.org/10.1021/ja4006578.
[21] P.A. Rudd, S. Liu, L. Gagliardi, V.G.Jr. Young, C.C. Lu, Metal–Alane Adducts with Zero-Valent Nickel, Cobalt, and Iron, J. Am. Chem. Soc. 133 (2011) 20724–20727. https://doi.org/10.1021/ja2099744.
[22] R.C. Cammarota, C.C. Lu, Tuning Nickel with Lewis Acidic Group 13 Metalloligands for Catalytic Olefin Hydrogenation, J. Am. Chem. Soc. 137 (2015) 12486–12489. https://doi.org/10.1021/jacs.5b08313.
[23] J.T. Moore, N.E. Smith, C.C. Lu, Structure and dynamic NMR behavior of rhodium complexes supported by Lewis acidic group 13 metallatranes, Dalton Trans. 46 (2017) 5689–5701. https://doi.org/10.1039/C6DT04769F.
[24] J.Jr. Fajardo, J.C. Peters, Tripodal P3XFe–N2 Complexes (X = B, Al, Ga): Effect of the Apical Atom on Bonding, Electronic Structure, and Catalytic N2-to-NH3 Conversion, Inorg. Chem. 60 (2021) 1220–1227. https://doi.org/10.1021/acs.inorgchem.0c03354.
[25] J.B. Bonanno, T.P. Henry, P.T. Wolczanski, A.W. Pierpont, T.R. Cundari, Evidence for Strong Tantalum-to-Boron Dative Interactions in (silox)3Ta(BH3) and (silox)3Ta(η2-B,Cl-BCl2Ph) (silox = tBu3SiO)1, Inorg. Chem. 46 (2007) 1222–1232. https://doi.org/10.1021/ic0616885.
[26] M. Sircoglou, N. Saffon, K. Miqueu, G. Bouhadir, D. Bourissou, Activation of M–Cl Bonds with Phosphine–Alanes: Preparation and Characterization of Zwitterionic Gold and Copper Complexes, Organometallics 32 (2013) 6780–6784. https://doi.org/10.1021/om4005884.
[27] M. Sircoglou, M. Mercy, N. Saffon, Y. Coppel, G. Bouhadir, L. Maron, D. Bourissou, Gold(I) Complexes of Phosphanyl Gallanes: From Interconverting to Separable Coordination Isomers, Angewandte Chemie International Edition 48 (2009) 3454–3457. https://doi.org/10.1002/anie.200900737.
[28] E.J. Derrah, M. Sircoglou, M. Mercy, S. Ladeira, G. Bouhadir, K. Miqueu, L. Maron, D. Bourissou, Original Transition Metal→Indium Interactions upon Coordination of a Triphosphine−Indane, Organometallics 30 (2011) 657–660. https://doi.org/10.1021/om1011769.

[29] Q. Lai, M.N. Cosio, O.V. Ozerov, Ni complexes of an alane/tris(phosphine) ligand built around a strongly Lewis acidic tris(N-pyrrolyl)aluminum, Chem. Commun. 56 (2020) 14845–14848. https://doi.org/10.1039/D0CC05452F.
[30] Q. Lai, N. Bhuvanesh, J. Zhou, O.V. Ozerov, Formation of an Ag→Al dative bond is avoided in reactions of an alane/tris(phosphine) ligand with monovalent silver, Dalton Trans. 50 (2021) 5776–5778. https://doi.org/10.1039/D1DT01068A.
[31] B. E. Mann, A. Musco, A 31 P nuclear magnetic resonance investigation of the structure, equilibria, and kinetics of [Pt(PR 3) n] in solution, Journal of the Chemical Society, Dalton Transactions 0 (1980) 776–785. https://doi.org/10.1039/DT9800000776.
[32] A. Sen, J. Halpern, Aspects of the low-temperature chemistry of tris(triphenylphosphine)platinum(0), Inorg. Chem. 19 (1980) 1073–1075. https://doi.org/10.1021/ic50206a061.
[33] H. Braunschweig, K. Gruss, K. Radacki, Interaction between d- and p-Block Metals: Synthesis and Structure of Platinum–Alane Adducts, Angewandte Chemie International Edition 46 (2007) 7782–7784. https://doi.org/10.1002/anie.200702726.
[34] J. Bauer, R. Bertermann, H. Braunschweig, K. Gruss, F. Hupp, T. Kramer, New Metal-Only Lewis Pairs: Elucidating the Electronic Influence of N-Heterocyclic Carbenes and Phosphines on the Dative Pt-Al Bond, Inorg. Chem. 51 (2012) 5617–5626. https://doi.org/10.1021/ic300531b.
[35] P. Brueggeller, Synthesis and phosphorus-31 NMR studies of five-coordinate platinum(II) complexes of tris(2-(diphenylphosphino)ethyl)phosphine and monodentate phosphorus ligands, Inorg. Chem. 26 (1987) 4125–4127. https://doi.org/10.1021/ic00271a032.
[36] P. Chini, G. Longoni, Improved synthesis of mononuclear platinum(0) compounds which contain tertiary phosphines and carbon monoxide, Journal of the Chemical Society A: Inorganic, Physical, Theoretical 0 (1970) 1542–1546. https://doi.org/10.1039/J19700001542.
[37] J. Browning, P.L. Goggin, R.J. Goodfellow, M.G. Norton, A.J.M. Rattray, B.F. Taylor, J. Mink, Vibrational and nuclear magnetic resonance spectroscopic studies on some carbonyl complexes of gold, palladium, platinum, rhodium, and iridium, J. Chem. Soc., Dalton Trans. (1977) 2061–2067. https://doi.org/10.1039/DT9770002061.
[38] A.C. Smithies, M. Rycheck, M. Orchin, The preparation and properties of some *cis*-platinum(II) carbonylphosphine complexes, PtX2(CO)(PR3), Journal of Organometallic Chemistry 12 (1968) 199–202. https://doi.org/10.1016/S0022-328X(00)90913-6.
[39] D.G. Gusev, J.U. Notheis, J.R. Rambo, B.E. Hauger, O. Eisenstein, K.G. Caulton, Characterization of PtH3(PtBu3)2+ as the First Dihydrogen Complex of d8, Pt(II), J. Am. Chem. Soc. 116 (1994) 7409–7410. https://doi.org/10.1021/ja00095a055.
[40] S.S. Stahl, J.A. Labinger, J.E. Bercaw, Investigations of the Factors Affecting the Stability of Dihydrogen Adducts of Platinum(II), Inorg. Chem. 37 (1998) 2422–2431. https://doi.org/10.1021/ic970944y.
[41] B.F.M. Kimmich, R.M. Bullock, Protonation of (PCP)PtH To Give a Dihydrogen Complex, Organometallics 21 (2002) 1504–1507. https://doi.org/10.1021/om0108651.
[42] O. Rivada-Wheelaghan, M. Roselló-Merino, M.A. Ortuño, P. Vidossich, E. Gutiérrez-Puebla, A. Lledós, S. Conejero, Reactivity of Coordinatively Unsaturated Bis(N-heterocyclic carbene) Pt(II) Complexes toward H2. Crystal Structure of a 14-Electron Pt(II) Hydride Complex, Inorg. Chem. 53 (2014) 4257–4268. https://doi.org/10.1021/ic500705t.

[43] R.H. Crabtree, Dihydrogen Complexation, Chem. Rev. 116 (2016) 8750–8769. https://doi.org/10.1021/acs.chemrev.6b00037.
[44] G. Sean McGrady, G. Guilera, The multifarious world of transition metal hydrides, Chemical Society Reviews 32 (2003) 383–392. https://doi.org/10.1039/B207999M.
[45] M.D. Butts, B.L. Scott, G.J. Kubas, Syntheses and Structures of Alkyl and Aryl Halide Complexes of the Type [(PiPr3)2PtH(η1-XR)]BArf and Analogues with Et2O, THF, and H2 Ligands. Halide-to-Metal π Bonding in Halocarbon Complexes, J. Am. Chem. Soc. 118 (1996) 11831–11843. https://doi.org/10.1021/ja961836y.
[46] M.M. Deegan, K.I. Hannoun, J.C. Peters, Dihydrogen Adduct (Co–H2) Complexes Displaying H-Atom and Hydride Transfer, Angewandte Chemie International Edition 59 (2020) 22631–22637. https://doi.org/10.1002/anie.202009814.
[47] S.S. Batsanov, Van der Waals Radii of Elements, Inorganic Materials 37 (2001) 871–885. https://doi.org/10.1023/A:1011625728803.
[48] B. Cordero, V. Gómez, A. E. Platero-Prats, M. Revés, J. Echeverría, E. Cremades, F. Barragán, S. Alvarez, Covalent radii revisited, Dalton Transactions 0 (2008) 2832–2838. https://doi.org/10.1039/B801115J.
[49] W. Gu, B.J. McCulloch, J.H. Reibenspies, O.V. Ozerov, Improved methods for the halogenation of the [HCB11H11]− anion, Chem. Commun. 46 (2010) 2820–2822. https://doi.org/10.1039/C001555E.
[50] APEX4 Software / Chemical Crystallography, (n.d.). https://www.brukersupport.com/ProductDetail/9269 (accessed April 14, 2024).
[51] SAINT Version 8.40B and SADABS, Bruker Analytical X-Ray Systems Inc., Madison, Wisconsin, USA (2012).
[52] G.M. Sheldrick, SHELXT – Integrated space-group and crystal-structure determination, Acta Cryst A 71 (2015) 3–8. https://doi.org/10.1107/S2053273314026370.
[53] G.M. Sheldrick, A short history of SHELX, Acta Cryst A 64 (2008) 112–122. https://doi.org/10.1107/S0108767307043930.

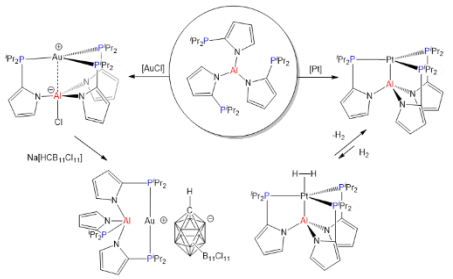
[AuCl]
[Pt]
Na[HCB11Cl11]
-H2
H2